Molecular Crystals and Liquid Crystals
Publication details, including instructions for authors and subscription information:
http://www.tandfonline.com/loi/gmcl16

Heat Capacity of the Discotic Mesogen, 2,3,6,7,10,11-Hexa-n octanoyloxy triphenylene: A Complex Solid State Polymorphismt

Gerald R. Van Hecke [a b] , Kazutoshi Kaji [a] & Michio Sorai [a]

[a] Chemical Thermodynamics Laboratory, Faculty of Science, Osaka University, Toyonaka, Osaka, 560, Japan

[b] Department of Chemistry, Harvey Mudd College, Claremont, CA, U.S.A. 91711

Version of record first published: 20 Apr 2011.

To cite this article: Gerald R. Van Hecke , Kazutoshi Kaji & Michio Sorai (1986): Heat Capacity of the Discotic Mesogen, 2,3,6,7,10,11-Hexa-n octanoyloxy triphenylene: A Complex Solid State Polymorphismt, Molecular Crystals and Liquid Crystals, 136:2-4, 197-220

To link to this article: http://dx.doi.org/10.1080/00268948608074727

Mol. Cryst. Liq. Cryst., 1986, Vol. 136, pp. 197–219
0026-8941/86/1364–0197/$25.00/0

Printed in the United States of America

Heat Capacity of the Discotic Mesogen, 2,3,6,7,10,11-Hexa-*n*-octanoyloxy triphenylene: A Complex Solid State Polymorphism†

GERALD R. VAN HECKE,‡ KAZUTOSHI KAJI and MICHIO SORAI

Chemical Thermodynamics Laboratory, Faculty of Science, Osaka University, Toyonaka, Osaka 560, Japan

(*Received December 9, 1985*)

Heat capacity of the discotic mesogen, 2,3,6,7,10,11-hexa-*n*-octanoyloxy triphenylene (HAT-C8) has been measured between 12 and 425 K by adiabatic calorimetry. HAT-C8 exhibited a variety of melting phenomena depending on its thermal history. The solids well annealed at around 361 and 349 K melted at 362.6 and 359.7 K, respectively, while a fresh sample obtained by recrystallization from an ethanol solution melted at 348 K. These three solid modifications have been here designated as solids I, II and III in the order of higher melting point. The enthalpy and entropy of melting for the solids I, II and III were 24.21 kJ mol^{-1}/66.76 J K^{-1} mol^{-1}, 25.44/71.12 and 34.77/99.91, respectively: the lower the melting point is, the larger the melting entropy is. The transition from the columnar mesophase to isotropic liquid occurred at 402.16 K accompanied by enthalpy and entropy changes of 3.626 kJ mol^{-1} and 9.02 J K^{-1} mol^{-1}. All the solid forms obeyed the third law of thermodynamics: that is, no residual entropies at 0 K within the present experimental error. A surprising fact is that the solid III, characterized by the lowest melting point among the three, is the most stable crystalline phase at 0 K. Its Gibbs free energy crosses over those of the solids I and II at around 290 K, although the present calorimetric study failed to realize completely this phase transition. The expected entropy associated with this hidden transition is as large as 52.8 J K^{-1} mol^{-1}. Some reasons for the unsuccessful observation of this transition have been discussed in relation to different molecular conformations in each solid phase. The thermal behavior of HAT-C8 has been compared with that of the benzene-core discotic mesogen having the same alkyl chains. A remarkable difference is that the entropy gain due to the transition from the columnar phase to the isotropic liquid is extremely small for HAT-C8 (9.02 J K^{-1} mol^{-1}) in comparison with the benzene-core (59.93 J K^{-1} mol^{-1}).

Keywords: heat-capacity, discotic triphenylene, polymorphism

† Contribution No. 88 from the Chemical Thermodynamics Laboratory.

‡ Permanent address: Department of Chemistry, Harvey Mudd College, Claremont, CA, U.S.A. 91711.

INTRODUCTION

At this writing many examples of disc-shaped molecules that exhibit liquid crystalline phases are well known.[1–8] Various, though not numerous, physical studies have been performed on some of these discotic materials forming columnar mesophases and most of these studies have been made on the first of the discotic mesogens, the hexasubstituted benzenes.[9] Closely following the discovery of the benzene core discotic materials[1] was the discovery of the triphenylene series.[2] Since that time discotic molecules have been formed derivatizing truxene,[3] rufigallol,[4] trioxatruxene,[5] trithiatruxene,[6] naphtalene,[7] and even cyclohexane.[8] The columnar mesophases exhibited by these various derivatives are many and varied, and, of course, raise many questions as to relationships between their physical properties. Earlier work in these laboratories elucidated the thermal properties of some members of the hexasubstituted benzene discotic materials. The thermal measurements on hexa-*n*-hexanoyloxy,[10] -*n*-heptanoyloxy,[11] -*n*-octanoyloxybenzene[12] yielded several interesting results including the surprising observation that the heat capacity of the columnar phase was less than that of the solid and isotropic phases that proceed and follow it respectively in temperature. Also a rich solid state polymorphism was observed for these materials. However, only one type of mesophase is observed in these compounds, in contrast to various triphenylene derivatives where the first examples of polymorphism in the types of columnar phases were observed. An important, motivating question for us was, what are the thermal properties of polymorphic columnar phases? We report here the results of adiabatic calorimetry and infra-red spectral studies on the hexa-*n*-octanoyloxy derivative of triphenylene. As reported in the literature, we observed in this material only one columnar mesophase but in contrast to the literature, we found a complex solid state polymorphism. Other derivatives that exhibit polymorphic columnar mesophases will be the subject of future works.

EXPERIMENTAL

Sample preparation

2,3,6,7,10,11-hexa-*n*-octanoyloxytriphenylene, herein called HAT-C8, was prepared by various modifications of literature reports.[2,13–15] Briefly, the synthetic steps were the condensation of veratrole to

hexamethoxytriphenylene using the Lewis acid ferric chloride,[13] demethoxylation to the hexahydroxytriphenylene using boron tribromide,[14,15] and finally condensation of octanoic acid chloride with the hexahydroxytriphenylene in pyridine to yield the hexaester product. Repeated syntheses netted various batches whose total was upwards of 15 g of product. The combined reaction yields, each of which had been recrystallized from ethanol at least three times, were recrystallized again from ethanol. This recrystallized sample was dried in vacuo until a constant weight was obtained.

Thermal analysis

Preliminary observations of thermal properties were made using a home-built differential thermal analysis (DTA) apparatus and a differential scanning calorimeter (DSC) (a Thermal Analyzer DT-30, Shimadzu Corp.) in the range 80–420 K. The mass of specimen used for the DTA and DSC probes was about 100 mg and 10 mg, respectively.

Heat capacity measurements

Heat capacities in the range 12 K to 425 K were measured wtih an adiabatic calorimeter.[16] The calorimeter cell was made of gold-plated copper and had inner volume of 10 cm^3. Temperature of the calorimeter cell was measured with a platinum resistance thermometer (Minco Products, Inc., Model S1055-2) whose temperature scale had been calibrated on the basis of the IPTS-68. To perform the various measurements, we twice loaded the calorimeter cell with the sample. In the first case, the cell was filled to 80% of its total volume by repeating a load-melt-freeze-load cycle of sample addition. The amount of sample charged was 0.00831871 mol (= 8.9965 g after a buoyancy correction assuming a sample density of 1.12 g cm^{-3}). In the second case, the calorimeter cell was loaded with a powdered sample that was not melted and whose mass was 4.1927 g (= 0.00387683 mol). In both cases, a small amount of helium gas (100 Torr) was sealed in the cell to aid the heat transfer.

Infrared absorption spectroscopy

Variable-temperature IR spectra were recorded for Nujol mulls between 103 and 414 K with an Infrared Spectrophotometer Model DS-402G (Japan Spectroscopic Co., Ltd.) in the range 4000–400 cm^{-1}.

RESULTS AND DISCUSSION

Our thermal studies have elucidated a much more complex phase behavior for HAT-C8 than first suggested in the literature.[2] For example, the reported m.p. is 66 °C, which we believe is actually the m.p. of a metastable crystal. As implied above HAT-C8 exhibited a variety of melting phenomena depending on its thermal history. Fresh sample obtained by recrystallization from an ethanol solution melted at 70 °C while crystals obtained from melt gave varying results. With rapid cooling (> 5 °C/min), undercooled columnar mesophase crystallized into a solid that melted at either 61 or 70 °C. On the other hand, the crystal obtained by slowly cooling the mesophase melted at 81 °C. We thought, at this point, that this crystal modification was the most stable solid form and the others were metastable ones.

In order to obtain a pure phase of the stable crystal, that is, one not mixed with any other crystal forms, the sample in the adiabatic calorimeter was heated to 76 °C, five Kelvin below its melting point, and annealed there until the heat evolution due to the crystallization ceased. Then the sample was slowly cooled and further checked for thermal equilibrium at various temperatures. Heat capacity measurements for the specimen thus treated were then made between 12 and 425 K. The results were evaluated in terms of C_p, the molar heat capacity under constant pressure. The experimental data for the solid state are listed in Table I and those for the columnar mesophase (*D*) and isotropic liquid (*IL*) are given in Table II. For the reason described below, we shall designate this crystalline modification as "solid II".

As shown in Figure 1, the solid II exhibited three C_p anomalies with maxima at 237, 263 and 305 K. With increasing temperature, the melting of solid II is described by a "broad" melting peak centered

TABLE I

Molar heat capacity of HAT-C8 (solid-II)

$\frac{T}{\text{K}}$	$\frac{C_p}{\text{J K}^{-1}\text{ mol}^{-1}}$	$\frac{T}{\text{K}}$	$\frac{C_p}{\text{J K}^{-1}\text{ mol}^{-1}}$	$\frac{T}{\text{K}}$	$\frac{C_p}{\text{J K}^{-1}\text{ mol}^{-1}}$
13.864	48.14	128.787	805.33	257.673	1769.0
14.434	52.89	131.84	821.20	278.072	1776.2
15.099	58.03	134.95	836.93	280.463	1790.3
16.492	68.25	138.131	853.54	285.097	1827.2
17.169	73.50	141.299	869.39	287.223	1855.0
18.561	85.18	144.457	886.61	289.599	1882.9

TABLE I (*continued*)

$\frac{T}{K}$	$\frac{C_p}{J\ K^{-1}\ mol^{-1}}$	$\frac{T}{K}$	$\frac{C_p}{J\ K^{-1}\ mol^{-1}}$	$\frac{T}{K}$	$\frac{C_p}{J\ K^{-1}\ mol^{-1}}$
19.283	91.39	147.613	904.07	291.961	1916.1
20.019	98.09	150.768	922.95	294.329	1954.5
21.136	107.56	153.880	941.44	296.700	2008.5
22.584	120.54	156.952	959.10	299.036	2082.0
23.450	128.31	160.042	978.17	301.094	2159.8
24.482	137.58	163.149	997.96	302.884	2230.7
25.546	146.89	166.214	1018.4	304.653	2254.1
26.551	155.66	169.241	1039.3	306.428	2194.5
27.524	164.27	170.397	1045.8	308.238	2130.1
28.485	172.86	173.358	1068.7	310.309	2082.0
30.078	187.15	176.384	1091.0	312.700	2049.7
31.457	199.22	179.407	1113.2	315.197	2034.8
32.793	210.91	182.420	1135.6	317.914	2025.2
34.216	223.45	185.421	1158.7	321.025	2018.4
35.709	236.27	188.421	1182.3	326.417	2009.1
37.274	249.37	191.421	1206.2	327.859	2008.8
39.082	264.65	194.428	1229.1	330.020	2014.3
40.981	280.21	197.458	1253.3	333.608	2026.2
42.777	294.78	200.514	1279.3	337.908	2043.4
44.787	310.53	203.606	1305.3	342.187	2061.8
47.132	328.83	207.052	1330.4	346.432	2091.4
49.484	347.40	210.098	1358.6	349.912	2182.5
51.686	363.53	213.171	1385.2	351.752	2344.1
53.866	379.93	216.278	1413.2	352.447	2354.7
56.084	395.94	219.408	1441.0	352.906	2417.7
58.351	411.64	222.527	1474.0	353.356	2514.4
60.720	428.67	225.354	1502.6	353.795	2630.4
63.219	445.89	227.891	1534.4	354.220	2776.5
65.842	462.96	229.901	1556.2	354.630	2932.1
68.518	479.57	231.395	1574.2	355.018	3308.0
71.213	496.00	233.123	1598.8	355.386	3399.1
73.886	512.27	235.084	1615.3	355.741	3676.5
76.601	528.49	237.055	1624.0	356.077	3995.8
80.430	550.73	239.025	1621.1	356.393	4353.3
83.858	570.70	240.970	1615.9	356.732	4916.5
86.981	588.36	242.914	1616.5	357.093	5362.6
90.007	604.84	244.854	1623.8	357.431	5794.8
93.199	622.33	246.787	1633.2	357.750	6197.5
96.554	640.06	250.587	1658.5	358.055	6538.6
100.186	659.97	252.486	1688.8	358.347	6855.8
103.007	672.27	254.389	1717.1	358.628	7186.8
105.338	686.05	256.297	1744.2	358.900	7411.9
108.396	701.70	258.186	1769.8	359.277	8408.4
111.418	716.92	263.114	1814.9	359.779	7689.8
114.493	732.75	264.966	1800.8	360.380	5539.2
117.625	748.72	266.824	1782.6	361.380	3008.1
120.727	764.34	268.715	1772.3	362.838	2223.0
123.776	780.27	270.871	1768.7	364.462	2098.2
126.468	792.20	273.270	1765.1	366.114	2102.8

TABLE II

Molar heat capacity of HAT-C8 (discotic phase and isotropic liquid)

$\frac{T}{K}$	$\frac{C_p}{J\ K^{-1}\ mol^{-1}}$	$\frac{T}{K}$	$\frac{C_p}{J\ K^{-1}\ mol^{-1}}$	$\frac{T}{K}$	$\frac{C_p}{J\ K^{-1}\ mol^{-1}}$
344.605	2037.7*	389.869	2175.8	402.342	6004.2
346.821	2044.7*	394.310	2189.9	402.450	4469.6
349.768	2052.3*	397.999	2203.5	402.609	3313.7
352.707	2061.4*	399.722	2205.0	402.891	2381.0
355.638	2071.4*	400.040	2235.5	403.265	2268.6
358.603	2079.3*	400.355	2226.3	403.709	2269.9
361.601	2088.8*	400.669	2240.0	404.464	2269.7
364.591	2097.9	400.979	2351.4	405.465	2272.8
367.573	2106.0	401.270	2728.4	407.604	2285.8
369.579	2113.3	401.527	3548.8	409.811	2295.9
372.054	2120.9	401.743	4481.4	413.447	2309.9
374.271	2125.0	401.928	5417.8	417.070	2325.7
377.220	2134.0	402.076	6381.7	419.954	2335.9
380.933	2146.8	402.164	7155.7	422.474	2342.4
385.408	2162.6	402.250	6704.2		

* The values are those for undercooled discotic phase below the melting point of solid-I.

at 359.7 K (= 86.5 °C). The transition from the *D* to *IL* phase took place at 402.16 K (= 129.01 °C). This type of "broad" melting is quite unusual unless we admit the existence of an extraordinary large amount of impurities. However, if we closely inspect the melting curve shown in Figure 2 by solid circles, we can perceive a shoulder on the low temperature side of the melting curve, suggesting that a solid-to-solid transition similar to the lower temperature anomalies might be superimposed on the "true" melting. To test this conjecture, we repeated the observation of the melting behavior for the samples carefully annealed at temperatures just at the shoulder. As a result, the "broad" melting peak not only split into two peaks at 358.4 and 360.3 K but also a third peak appeared at 362.5 K. These observations suggested the existence of another, more stable crystal modification than the solid II. We successfully obtained this most stable crystal form by annealing the specimen at around 361 K for three weeks. Heat capacity measurements for the specimen thus treated were made between 12 and 366 K. The results are listed in Table III and plotted in Figure 3 along with the C_p data of the *D* and *IL* phases. In what follows, we shall call this crystalline form "solid I". The solid I exhibited two anomalies at 267 and 309 K, and melted at 362.6 K (= 89.4 °C). The melting behavior is compared with that of the solid II in Figure 2. The former peak is obviously sharper than the latter

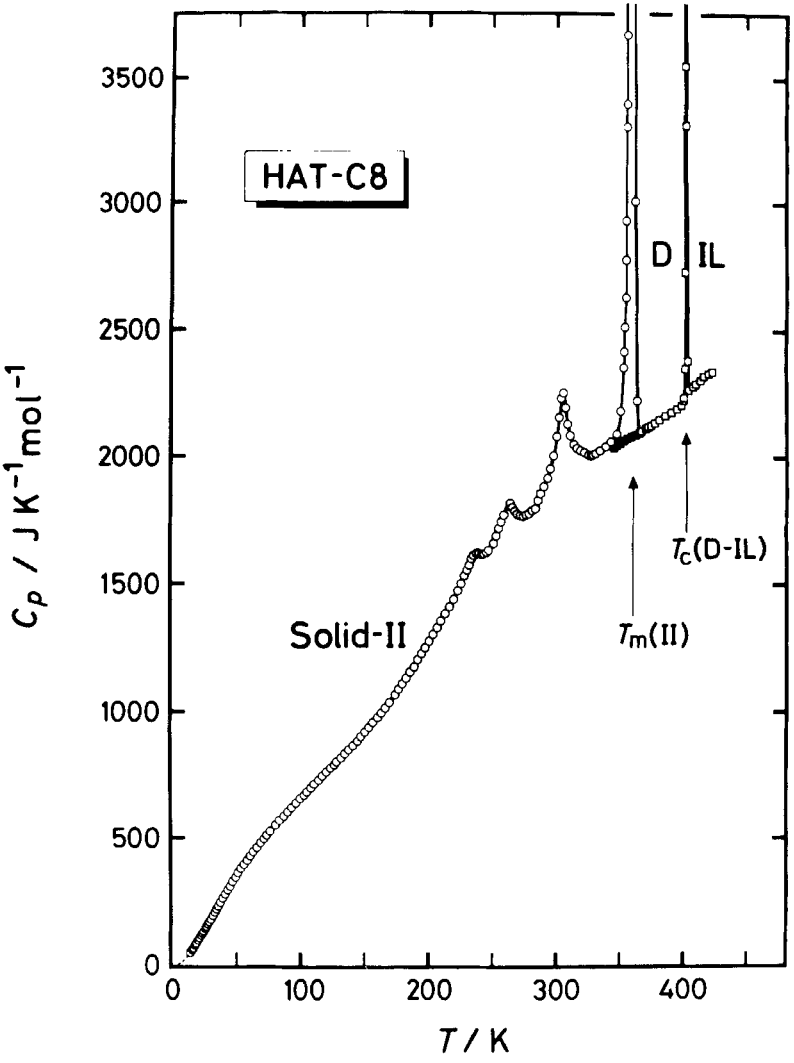

FIGURE 1 Molar heat capacity of HAT-C8 starting from the solid-II. In this and in Figures 3 and 4, "*D*" and "*IL*" indicate the discotic mesophase and the isotropic liquid phase, respectively. Undercooled *D*-phase is shown by solid squares.

one, indicating that the present sample does not contain a large amount of impurities.

In passing, it should be remarked here that although the columnar phase could be undercooled to 55 °C using the DTA and DSC techniques, in the adiabatic calorimeter we could only undercool the

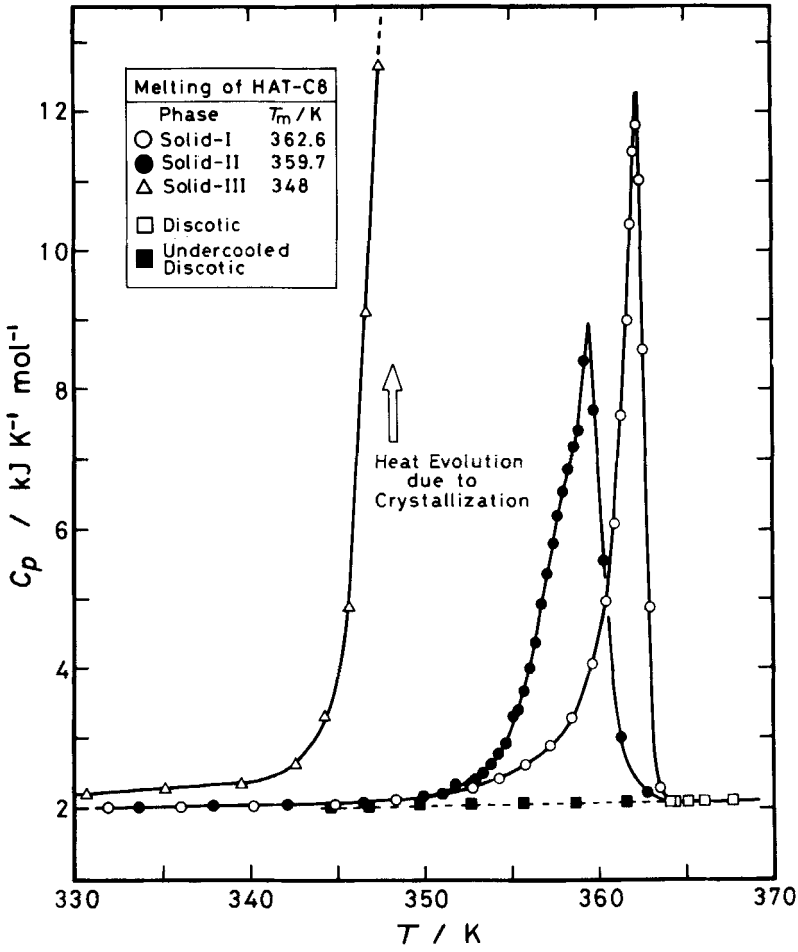

FIGURE 2 Molar heat capacities of the solids-I, II and III of HAT-C8 in the vicinity of their melting points.

columnar phase to 343 K (= 70 °C) which obviously limited the possible range of heat capacity measurements on the undercooled *D* phase. This is the case because adiabatic calorimetry is principally an equilibrium method and hence can sensitively detect a small change in temperature. The C_p data are listed in Table II and plotted in Figures 1–4 by solid squares.

For comparison, the heat capacity of the specimen, also recrystallized from EtOH but loaded in the calorimeter cell in a powdered form without melt, was measured from 12 K (see Table IV and

TABLE III

Molar heat capacity of HAT-C8 (solid-I)

T/K	C_p/J K^{-1} mol^{-1}	T/K	C_p/J K^{-1} mol^{-1}	T/K	C_p/J K^{-1} mol^{-1}
12.937	40.87	89.039	599.44	247.920	1676.7
13.434	44.09	92.240	616.99	250.968	1701.5
14.015	48.39	95.554	634.48	257.393	1759.4
14.713	53.49	99.010	652.15	260.628	1814.5
15.453	58.99	102.486	670.72	263.798	1876.3
16.235	64.79	105.753	685.47	266.910	1917.8
17.032	71.18	108.476	701.10	270.019	1878.6
17.793	77.37	112.059	719.75	273.164	1857.2
18.545	83.51	115.681	738.18	276.317	1852.3
19.328	90.41	119.325	756.75	282.567	1874.9
20.128	97.57	122.715	773.18	285.786	1892.2
20.912	104.58	125.642	788.48	289.051	1916.2
21.689	111.35	129.407	807.83	292.262	1945.9
22.467	118.21	133.049	826.58	295.459	1975.8
23.372	126.25	136.685	844.95	298.651	2016.6
24.380	135.22	140.309	863.85	301.805	2063.6
25.309	143.49	143.913	882.72	305.334	2122.8
26.315	152.30	147.541	902.86	309.275	2128.3
27.390	161.73	151.156	923.69	313.207	2099.3
28.394	170.66	154.405	936.05	317.174	2074.2
29.381	179.32	157.161	959.17	321.158	2060.3
30.358	187.88	160.741	980.49	323.659	2046.2
31.413	197.28	164.304	999.84	327.752	2034.9
32.748	209.15	167.832	1024.1	331.888	2025.1
34.338	222.99	171.359	1047.8	336.030	2022.6
35.999	237.25	174.864	1070.0	340.131	2037.3
37.720	251.32	178.318	1093.6	344.876	2051.8
39.813	268.01	182.538	1115.5	348.344	2135.1
42.110	285.40	185.171	1142.8	351.024	2212.1
44.296	303.79	188.700	1171.5	352.769	2295.2
46.425	319.16	192.192	1198.2	354.310	2427.0
48.527	338.16	195.573	1228.3	355.790	2623.5
50.811	355.88	197.616	1240.9	357.191	2890.0
53.293	373.48	200.898	1272.3	358.493	3288.2
55.880	391.91	204.132	1304.2	359.654	4056.1
58.380	408.89	207.364	1336.3	360.469	4965.9
60.805	426.83	210.609	1368.1	360.983	6086.2
63.225	442.86	213.811	1398.0	361.416	7616.0
65.569	457.74	216.958	1424.8	361.727	8979.8
67.949	472.46	220.071	1451.0	361.942	10385.
69.795	482.70	223.203	1476.6	362.136	11413.
71.637	494.53	226.759	1499.5	362.319	11800.
74.149	514.08	229.357	1526.2	362.505	11003.
76.737	525.22	232.449	1553.7	362.720	8572.5
79.449	541.65	235.559	1576.9	363.027	4867.4
80.320	547.30	238.697	1600.7	363.528	2282.5
82.873	563.04	241.803	1623.5	364.172	2095.7
85.991	582.10	244.876	1652.4	365.162	2097.7

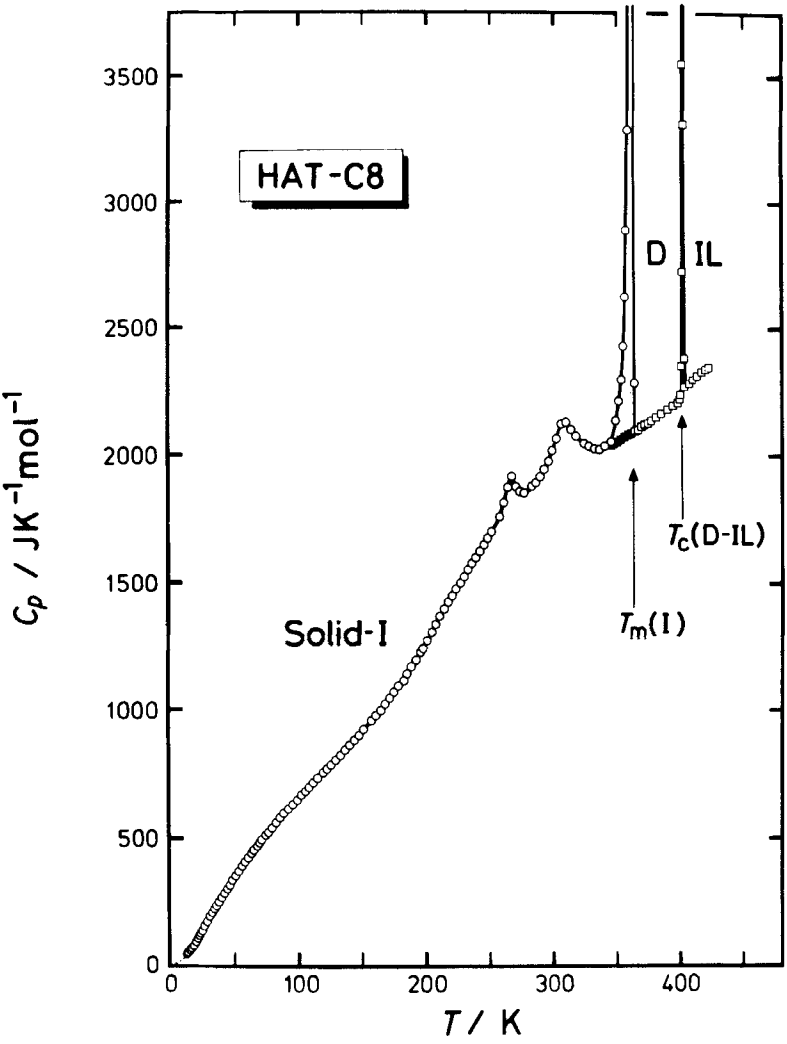

FIGURE 3 Molar heat capacity of HAT-C8 starting from the solid-I. Solid I was obtained from solid II by annealing the sample at 361 K for three weeks.

Figure 4). It should be remembered that previous runs were obtained on samples that while also recrystallized from EtOH, had been melted in order to pack and fill the calorimeter cell. This powder crystal modification will be designated as "solid III". As in the cases of the solids I and II, this solid III also exhibited C_p anomalies at 230 and 265 K. The heat capacity of the solid III was much smaller than those

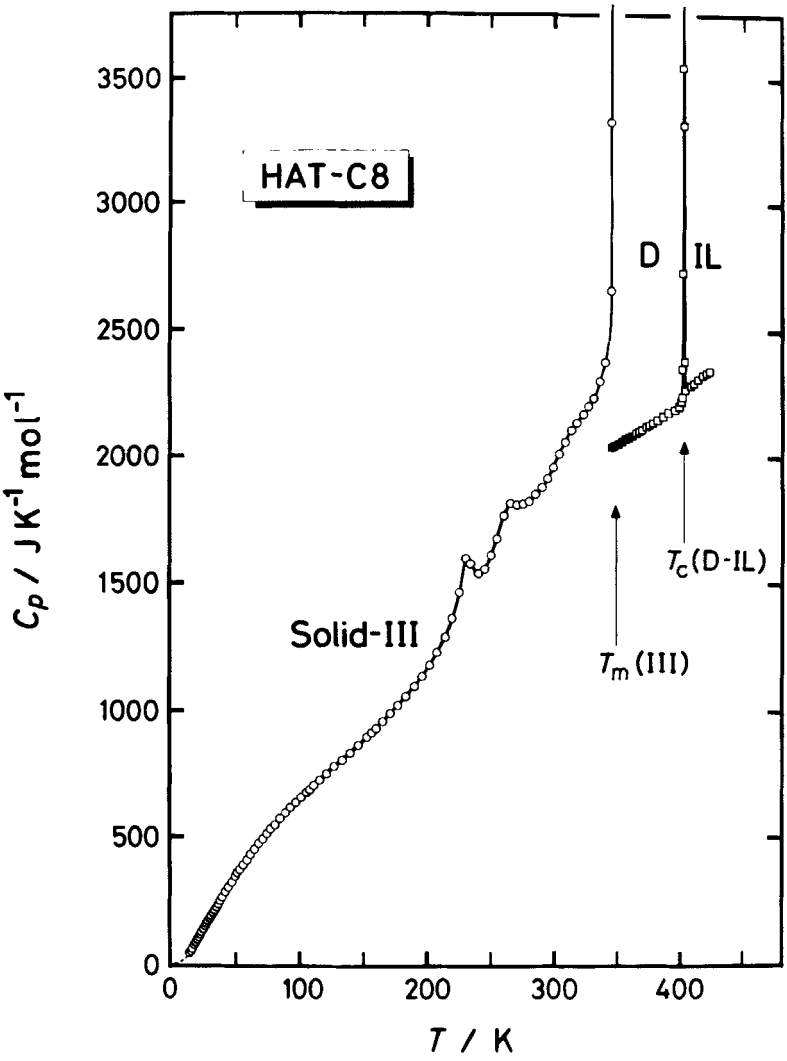

FIGURE 4 Molar heat capacity of HAT-C8 starting from the solid-III.

of the solids I and II below 310 K; for instance, the difference at 200 K amounted to 100 J K^{-1} mol^{-1}. This fact indicates that the molecules are closely packed in the crystal lattice of the solid III and the crystal is much harder than the solids I and II. The melting of the solid III began to occur at 342 K as noted a sharp rise in C_p which reached to 12.4 kJ K^{-1} mol^{-1} at 347.5 K. At this point, an exothermic temperature drift due to the crystallization to a more stable solid

TABLE IV

Molar heat capacity of HAT-C8 (solid-III)

T/K	C_p/J K^{-1} mol^{-1}	T/K	C_p/J K^{-1} mol^{-1}	T/K	C_p/J K^{-1} mol^{-1}
13.250	40.36	64.851	452.37	219.193	1366.3
14.142	47.15	68.083	473.24	224.776	1462.8
14.995	53.32	71.277	492.77	230.187	1598.5
15.880	59.82	74.457	512.07	233.546	1577.3
16.822	67.26	77.749	531.27	239.256	1537.8
17.862	75.82	81.094	547.90	244.456	1555.0
18.986	85.34	84.892	571.42	249.206	1611.0
20.154	96.39	89.097	594.35	254.403	1682.4
21.367	106.38	93.231	616.06	259.513	1764.4
22.605	116.97	97.362	635.90	264.518	1812.5
23.841	127.82	101.538	656.71	269.480	1806.7
25.076	138.07	105.765	676.81	274.422	1810.0
26.318	148.71	108.554	687.39	279.354	1821.2
27.508	158.88	111.342	704.64	284.258	1848.9
28.668	169.01	115.643	725.60	289.413	1878.7
29.850	179.27	120.967	749.81	293.684	1912.9
31.091	189.88	127.187	778.56	298.428	1956.1
32.391	201.00	133.351	806.05	303.155	2010.6
33.723	212.45	139.609	833.69	307.840	2058.4
34.957	222.81	145.963	862.69	312.489	2104.5
36.311	233.83	152.400	895.81	317.104	2135.6
37.944	246.83	156.649	914.28	322.038	2167.8
39.737	261.35	159.819	931.83	326.130	2202.4
42.057	282.12	165.029	959.49	330.651	2232.4
44.528	300.93	171.179	990.31	335.141	2300.0
47.097	320.19	177.253	1021.8	339.598	2374.3
49.744	342.09	183.392	1057.6	342.686	2655.8
51.673	358.70	189.619	1096.9	344.338	3327.2
53.566	370.91	195.796	1137.4	345.739	4903.5
56.225	390.34	201.653	1181.4	346.765	9125.3
58.978	408.96	207.616	1231.2	347.509	12416.
61.809	431.01	213.467	1291.2	(heat evolution)	

prevented us from further accurately measuring the heat capacity. However, we then followed the exothermic process keeping the cell in an adiabatic condition until the spontaneous warming ceased, at which time we supplied known amounts of Joule energy to the calorimeter cell and eventually raised the temperature of the specimen to 375.3114 K, which is a temperature in the D phase and is convenient for comparison of the molar enthalpies and entropies among the various solid modifications. In what follows, we shall designate this temperature as reference temperature T_{ref}.

As shown in Figure 2, the melting of the solid III was much sharper than those of the solids I and II. Table V summarizes the thermodynamic quantities associated with the melting of each solid modi-

TABLE V

Transition enthalpy and entropy of HAT-C8

Transition	T_{trs} / K	$\Delta_{trs}H$ / kJ mol^{-1}	$\Delta_{trs}S$ / J K^{-1} mol^{-1}
Solid-I → Discotic phase	362.6	24.21	66.76
Solid-II → Discotic phase	359.7	25.44	71.12
Solid-III → Discotic phase	348	34.77	99.91
Discotic phase → Isotropic liquid	402.16	3.626	9.02
not observed but expected phase transition			
Solid-III → Solid-I	~290	15.32	52.8

fication and the D to IL transition. Interestingly, the melting enthalpies and entropies increase remarkably in the order of the solids I < II < III.

In order to check whether the three solid forms obey the third law of thermodynamics, the molar entropies at T_{ref} were determined by integrating the C_p curve of each solid form and a part of the D phase with respect to ln T. The entropies below 12 K were estimated on the basis of an extrapolated heat capacity curve which was determined by the effective frequency distribution method.[17] As summarized in Table VI, the average value of the three molar entropies was (2399.4 ± 4.4) J K^{-1} mol^{-1} and the root-mean-square scattering was within the present experimental error of ±5.0 J K^{-1} mol^{-1}. In other words, each solid form has no residual entropy at zero Kelvin even though the crystal symmetry and the molecular packing in each of the three crystal forms are different.

In general when comparing crystalline polymorphs, a crystal with a higher melting point is more stable than one with a lower melting point. On this basis, the predicted order of stability of the solids I, II, III would appear to be solid I > II > III where I is most stable. In the present compound, however, the order is temperature dependent! The solid II is always actually less stable than the solid I, but the stability of the solid I vs solid III depends on temperatures as shown below. The molar enthalpies of the solids I and III at T_{ref} measured from their zero-point enthalpies are

$$H^\circ_{T_{ref}}(\mathrm{I}) - H^\circ_0(\mathrm{I}) = 473.70 \text{ kJ mol}^{-1}$$

and

$$H^\circ_{T_{ref}}(\mathrm{III}) - H^\circ_0(\mathrm{III}) = 479.67 \text{ kJ mol}^{-1}.$$

TABLE VI

Molar entropies of three solid phases of HAT-C8 at a reference temperature (= 375.3114 K)

Evaluated path	Molar entropy / J K^{-1} mol^{-1}
Solid-I + Discotic phase	2400.4
Solid-II + Discotic phase	2403.3
Solid-III + Discotic phase	2394.6
average	2399.4 ± 4.4
(experimental error is ±5.0)	

Since at T_{ref} HAT-C8 is in its columnar phase, the molar enthalpies at T_{ref} should be identical, that is,

$$H^{\circ}_{T_{ref}}(\mathrm{I}) = H^{\circ}_{T}\mathrm{H}^{\circ}_{T_{ref}} \quad (\mathrm{III}),$$

and the enthalpy difference between the two solids at 0 K amounts to

$$H^{\circ}_{0}(\mathrm{I}) - H^{\circ}_{0}(\mathrm{III}) = 5.97 \text{ kJ mol}^{-1}$$

Since the entropy term in the Gibbs energy has no contribution at 0 K, a difference between the two Gibbs energies just corresponds to the difference of the enthalpies at 0 K. The present estimate clearly indicates that the solid III is more stable by 5.97 kJ mol^{-1} than the solid I at 0 K in spite of its lower melting point. On the other hand, similar estimate for the solid II gives the following result, $H^{\circ}_{0}(\mathrm{II}) - H^{\circ}_{0}(\mathrm{III}) = 6.24$ kJ mol^{-1}. The order of crystal stability at 0 K is then III > I > II with III the most stable, while recall at 348 K the order is I > II > III. An important question is, then, when does solid III become more stable than solids I and II, that is, what are the cross-over temperatures? We estimated the Gibbs free energies for the solids I and III as a function of temperature with the results that the two Gibbs energy curves actually crossed at about 290 K. This situation is shown in Figure 5 in terms of $[G^{\circ}_{T} - G^{\circ}_{T}(\mathrm{III})]$ and $[H^{\circ}_{T} - H^{\circ}_{T}(\mathrm{III})]$. The Gibbs energy relationship among the various solid phases is schematically drawn in Figure 6, where solid IV refers to the least stable crystal modification recorded by DTA and DSC. No adiabatic calorimetric data was obtained on this form. As seen from Figures 5 and 6, the present calorimetric study determined that the solid III is the most stable crystal below 290 K while the solid I becomes the most stable above this temperature. While the transition of solid I to

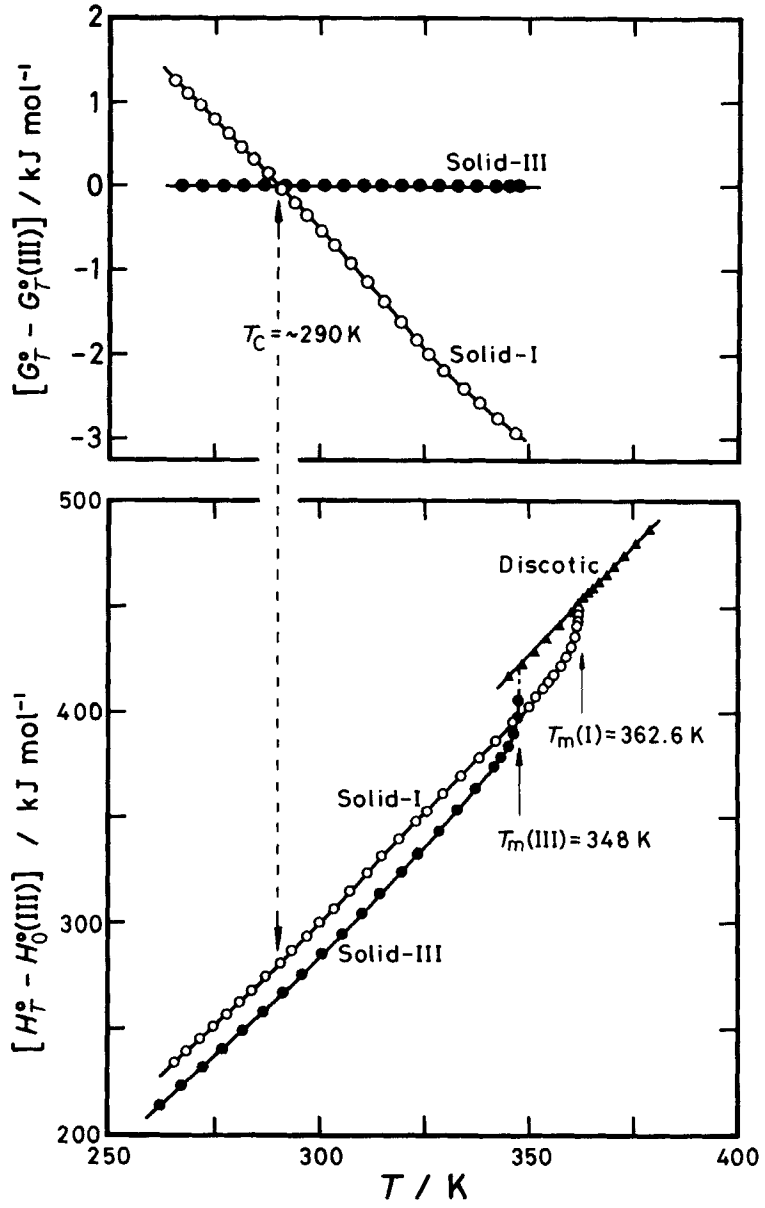

FIGURE 5 The Gibbs free energy relationship between the solids-I and III in terms of $[G_T^\circ - G_T^\circ(III)]$ (top) and the enthalpy relationship among the solids-I, III and the discotic phase in terms of $[H_T^\circ - H_0^\circ(III)]$ (bottom).

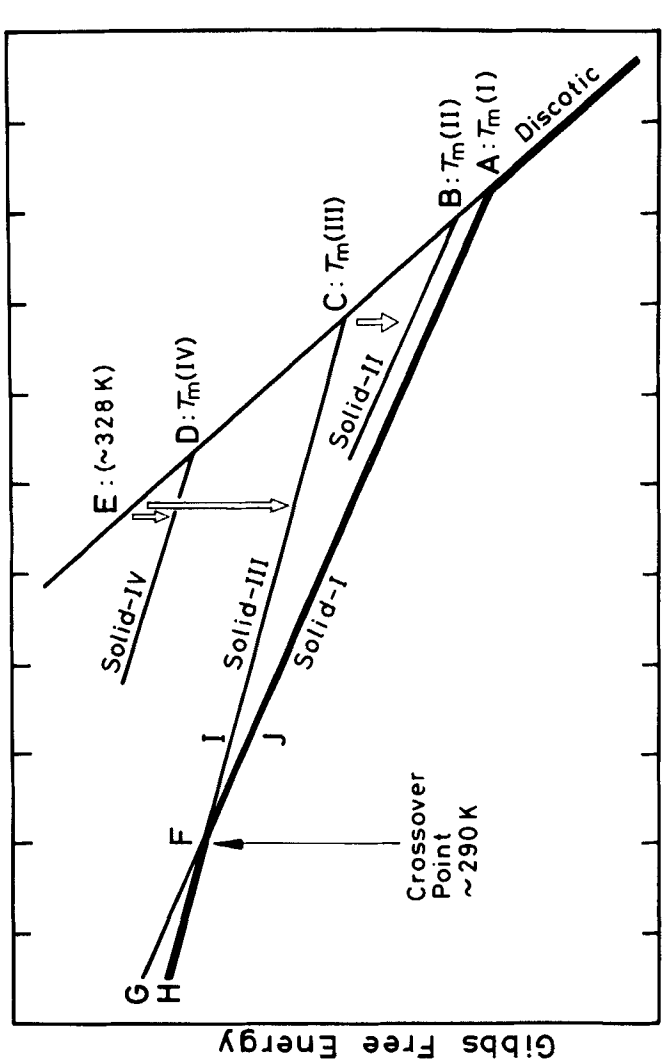

FIGURE 6 Schematic drawing of the Gibbs free energies of various phases in HAT-C8. A thick line corresponds to the most stable path although a phase transition at the crossover point "*F*" has not been observed. Arrows indicate spontaneous stabilization.

III is estimated to occur at 290 K, looking at Figure 6 it would appear that solid II to III would occur at some temperature greater than 290 K. A mystery is, however, why are these phase transitions, solid III to I and solid III to II, not observed around 290 K? If the transition of solid III to I did occur at 290 K, the transition enthalpy, $\Delta_{trs}H^\circ$, would amount to 15.32 kJ mol^{-1} ($= [H^\circ_{290}(I) - H^\circ_{290}(III)]$) and the transition entropy, $\Delta_{trs}S^\circ$, would be expected to be 52.8 J K^{-1} mol^{-1} ($= \Delta_{trs}H^\circ/290$). As shown in Table V, $\Delta_{trs}S^\circ$ corresponds to as much as 79% of the melting entropy for the solid I and 53% of that for the solid III.

In an attempt to observe the hidden phase transition at 290 K, we tried the following thermal treatment. First, the specimen in the *D* phase was cooled to 55 °C, the point labeled "*E*" in Figure 6, where crystallization occurred. After confirming that the crystal obtained was indeed the solid III, we cycled the temperature thirteen times between 240 and 300 K hoping that this procedure would facilitate the nucleation-and-growth of the solid I "embryo" in a medium of the solid III. The final results of heat capacity measurements on this sample in the range 202–345 K are shown in Figure 7 as solid circles. The C_p curve was substantially the same as that of the solid III except for a broad peak centered at 275 K which is indicated by an arrow in Figure 7. Even without definitive evidence, we believe that this broad peak includes a trace of the hidden phase transition. Disagreement of the transition temperature between the observed value (275 K) and the expected one (290 K) is not very significant because the cross-over point of the Gibbs energies is quite sensitive to small changes in the estimate of $[H^\circ_0(I) - H^\circ_0(III)]$. Even if the peak at 275 K were assigned to some, albeit faint, indication of the hidden phase transition, it is obvious that this transition is very difficult to realize.

Once the solid I is formed its Gibbs energy follows the path *G—F—J—A* shown in Figure 6, where we should point out that solid I is easily undercooled beyond the cross-over point "*F*". Similarly, once the solid III is formed, its Gibbs energy follows along the curve *H—F—I—C* and the solid III is easily superheated beyond the cross-over point "*F*" as well as the cross-over to solid II. One plausible reason why these phase transitions are not completely realized may originate in their extremely large transition entropies (52.8 J K^{-1} mol^{-1} for solid III to I for example). When the transition entropy due to a solid-to-solid phase transition is large, one can easily imagine that the crystal structure and the molecular conformation are very different between the high and low temperature phases.

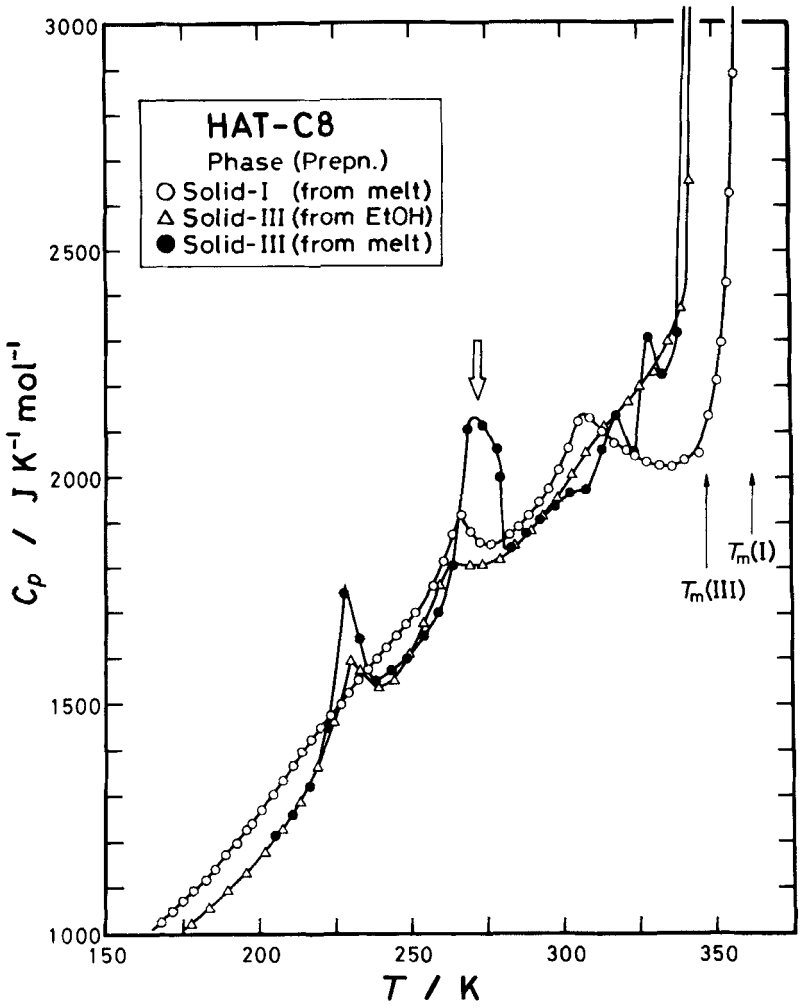

FIGURE 7 Comparison of molar heat capacities for the solids-I, III and the solid-III obtained from melt, which was subjected to temperature-cycling thirteen times between 240 and 300 K before heat capacity measurements. A peak indicated by an arrow seems to be a trace of the hidden phase transition from the solid-III to I.

Supporting the conjecture of the importance of molecular conformations are the infrared absorption spectra shown in Figures 8 and 9. For example compare a pair of the IR spectra obtained at 298 K: one recorded on a virginal crystal, that is, recrystallized powder not melted, the other recorded on a solid obtained by cooling its melt. Judging from the experience gained from previous heat treatments,

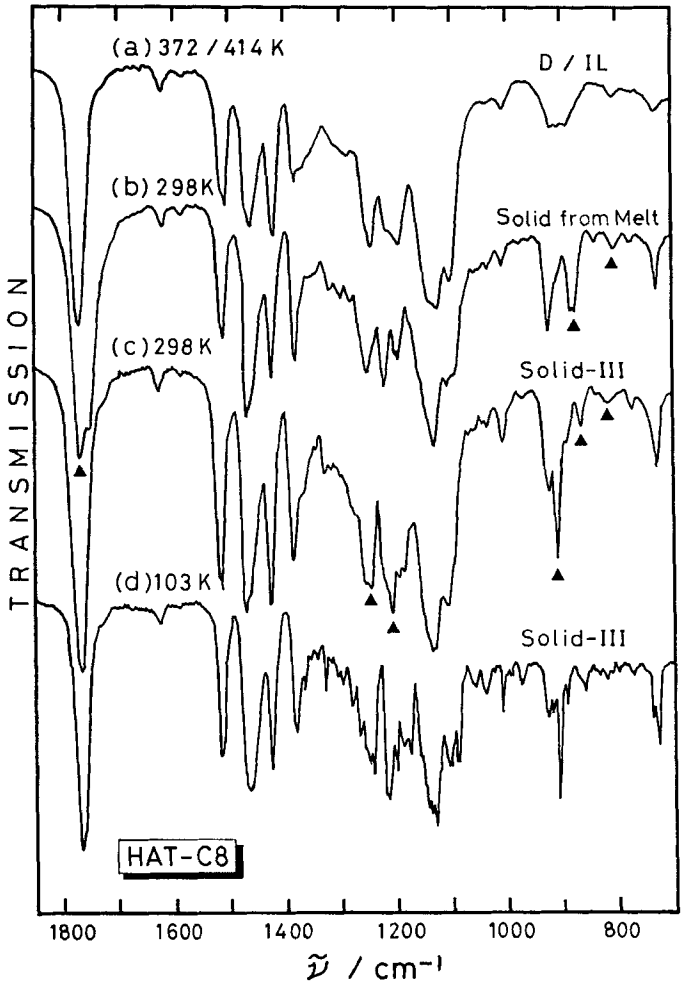

FIGURE 8 Infrared absorption spectra for HAT-C8 in the range 1800–700 cm^{-1}. In this and in Figure 9, the two spectra recorded at 298 K are quite different: one is a spectrum for a powdered specimen precipitated from an ethanol solution (the solid-III) and the other is a spectrum for the specimen obtained from melt (probably the solid-II). Characteristic bands showing remarkable difference between the two are labeled by solid triangles.

the solid form of the latter is probably the solid II which must have a free energy close to that of the solid I. All the IR bands showing noticeable differences between the two solids are marked by solid triangles. Of particular interest is the change in the strong C=O stretching band around 1765 cm^{-1}. This band is a singlet in

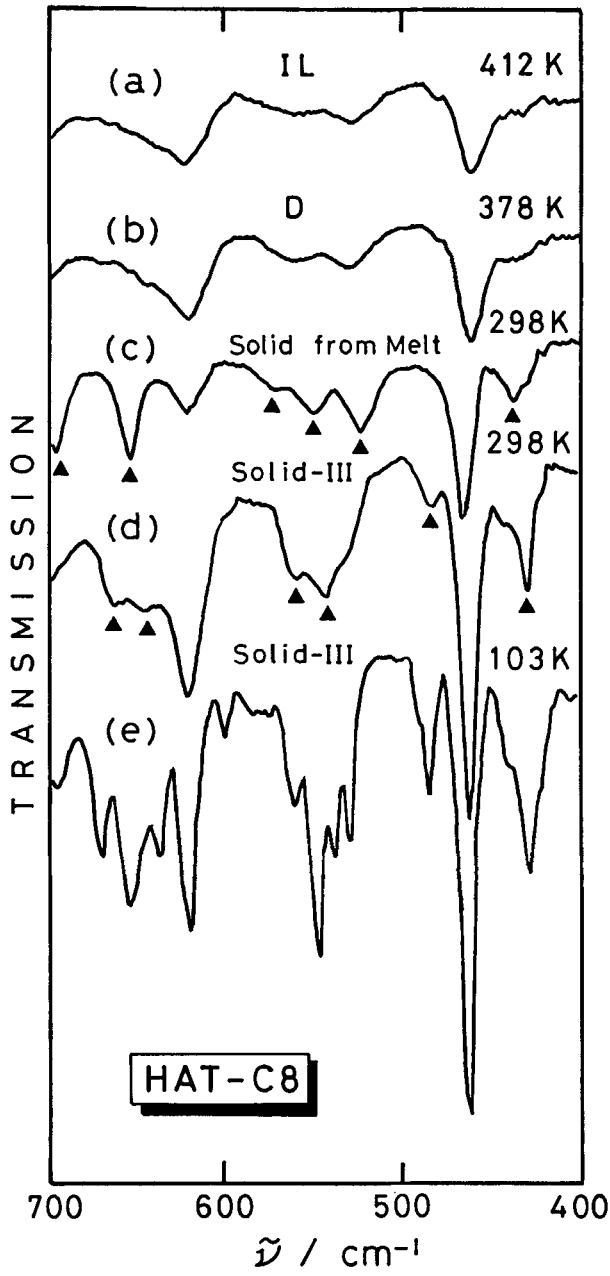

FIGURE 9 Infrared absorption spectra for HAT-C8 in the range 700–400 cm^{-1}.

the solid III and in the *D* and *IL* phases whereas it splits into doublet at 1767/1754 cm^{-1} in "the solid II". As discussed in a previous paper[10] describing a disc-like molecule having a benzene-core, this band is quite sensitive to crystal structuure and molecular motions. As postulated above, the solid III is a dense crystal compared with the solids I and II. If the present disc-like molecules are planar in the solid III, the six C=O groups of the molecule may be situated in a crystalline field similar to one another and hence the C=O stretching band would be expected to be the observed singlet. On the other hand, if the molecules form tightly bound pairs in the solid II (and in the solid I), the splitting of the C=O stretching band can easily be understood from a consideration of the crystalline field. In this case, six alkyl chains of a molecule are oriented upward and downward alternately and, as a whole, a molecule has a bulky structure.[18] If this is the case, the relevant phase transition involves drastic changes in the molecular conformations and it should come as no surprise that such rearrangements in the solid state would occur only with difficulty because of the high activation energy due to steric hindrance.

Comparing the present calorimetric results to those for the discotic mesogens having a benzene-core, we notice two interesting differences in characteristic thermal properties of the benzene-core discotic mesogens: (i) The existence of many solid-to-solid phase transition(s) each accompanied by a large transition entropy due to conformational melting of the alkyl moieties; (ii) The heat capacity of the columnar mesophase is smaller than those of the adjacent crystalline and isotropic liquid phases.[10–12,19]

Prior to discussion on the item (i), we should recall that if HAT-C8 follows the most stable Gibbs energy path during a temperature variation, then it should of course undergo the phase transition from the stable low-temperature phase (the solid III) to the stable high-temperature phase (the solid I) at around 290 K although this transition has not been clearly realized during the present experiments. In Figure 10 we plot the standard molar entropy (divided by temperature for convenient scaling) as a function of temperature for two compounds that exhibit columnar mesophases, HAT-C8 and, for the sake of comparison, benzene-hexa-*n*-octanoate (BH8 for short), a compound in which the triphenylene core of HAT-C8 is replaced by a benzene core. As in the case of BH8, HAT-C8 is characterized by a solid phase transition with a large entropy acquisition only if the hidden phase transition occurs. However, any of the melting entropies for the solids I, II and III, 66.76, 71.12 and 99.91 J K^{-1} mol^{-1} respectively, were much smaller than the 129.81 J K^{-1} mol^{-1} value

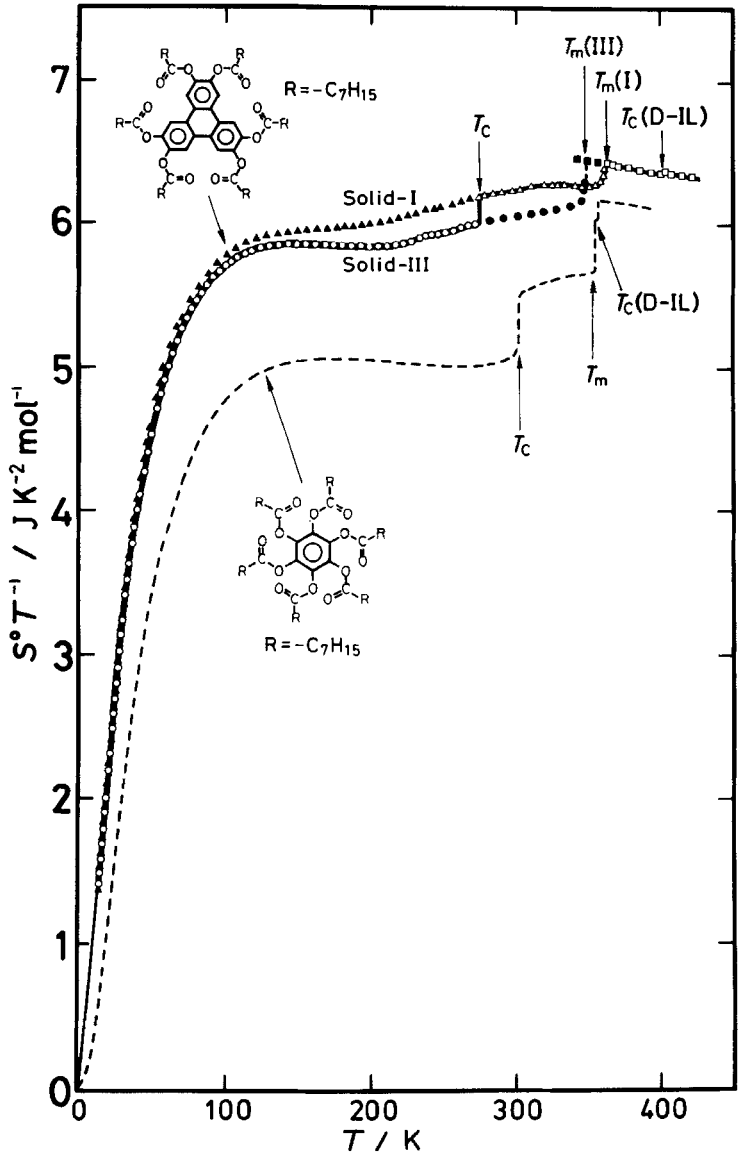

FIGURE 10 Temperature dependence of the standard molar entropies of HAT-C8. For convenience, the entropy is divided by temperature. △ and ▲: the solid-I, ○ and ●: the solid-III, □ and ■: the discotic and isotropic liquid phases of HAT-C8. The solid marks indicate the undercooled or superheated metastable states. A thick line passing through the open marks corresponds to the most stable path. The broken line is the molar entropy of BH8.[12]

observed for BH8. Moreover, the entropy change accompanying the *D* to *IL* transition in the present compound (9.02 J K^{-1} mol^{-1}) was extremely small compared with 59.93 and 53.77 J K^{-1} mol^{-1} for BH7 and BH8, respectively.[10-12,19] In other words, conformational melting of the alkyl-chains has proceeded to a greater extent in the crystalline and columnar phases of the triphenylene compound than in those of the benzene-core mesogens.

With regard to point (ii) above, the C_p values just below and above the melting point were nearly identical for the solids I and II while for the solid III the C_p decreased about 300 J K^{-1} mol^{-1} on going from the solid to the columnar phase. In the case of the benzene-core mesogens,[10-12,19] the C_p decrease was 100–180 J K^{-1} mol^{-1}. The size of the C_p decrease seems to be related to the extent of the conformational melting of the alkyl-chains in the solid and *D* phases, and hence the amount of the melting entropy. If the melting entropy is small, the C_p decrease is also small. In this respect, the large C_p decrease found for the solid III supports the above mentioned fact that the solid III is harder than the solids I and II and thus the molecules are of more ordered state in the former than in the latter. Similarly, the rather small C_p increase on going from the *D* to *IL* phase for the present compound can be associated with the small transition entropy in comparison with those for the benzene-core mesogens.

The origin of the C_p anomalies may be due to conformational changes or perhaps in some cases, reflections of the unobserved but expected transitions for solid III to I and solid III to II. However, the present triphenylene-core discotic mesogen exhibits a striking contrast to the benzene-core mesogens.[10-12,19] The conformational changes of the constituent alkyl chains occur as sharp solid-to-solid phase transitions (*s*) in the latter, while they appear as faint C_p anomalies in the former.

Acknowledgments

We wish to thank T. H. Smith, R. L. Cole, J. S. Oliver, M. J. Sailor, and A. Jacob for their synthesis of the compound. One of us (GRVH) wishes to thank Profs. H. Suga, M. Sorai and the members of the Chemical Thermodynamics Laboratory for their many hospitalities during his sabbatical visit.

References

1. S. Chandrasekhar, B. K. Sadshiva, K. A. Suresh, N. V. Madhusudana, S. Kumar, R. Shashidhar and G. Venkatesh, *J. de Phys.* (*Paris*) **40**, C3–120 (1979).

2. C. Destrade, M. C. Mondon and J. Malthete, *J. de Phys.*, (*Paris*), **40**, C3–17 (1979).
3. C. Destrade, J. Malthete, Huu Tinh Nguyen and H. Gasparoux, *Phys. Lett.*, **78A**, 82 (1980).
4. a. J. Billard, J. C. Dubois, R. Vaucher and A. M. Levelut, *Mol. Cryst. Liq. Cryst.*, **66**, 115 (1981).
b. P. Le Barney, J. Billard and J. C. Dubois, "*Liquid Crystals and Ordered Fluids*," Vol. 4, A. C. Griffin and J. F. Johnson, Eds.; Plenum Press: New York, p. 57 (1984).
5. Huu Tinh Nguyen, R. Cayuela, J. Malthete and C. Destrade, *Mol. Cryst. Liq. Cryst.*, in press: "Proceedings of the 10th International Liquid Crystal Conference," York, England (1984).
6. L. Mamlok, J. Malthete, Huu Tinh Nguyen, C. Destrade and A. M. Levelut, *J. Phys. Lett.*, (*Paris*), **43**, L-641 (1982).
7. D. M. Kok, H. Wynberg and W. H. De Jeu, *Mol. Cryst. Liq. Cryst.*, in press: "Proceedings of the 10th International Liquid Crystal Conference," York, England (1984).
8. B. Kohne and K. Praefcke, *Angew. Chem. Int. Ed.*, **23**, 82 (1984).
9. J. C. Dubois and J. Billard, "*Liquid Crystals and Ordered Fluids*," Vol. 4, A. C. Griffin and J. F. Johnson, Eds.; Plenum Press: New York, p. 1043 (1984).
10. M. Sorai, K. Tsuji, H. Suga and S. Seki, *Mol. Cryst. Liq. Cryst.*, **59**, 33 (1980).
11. M. Sorai and H. Suga, *Mol. Cryst. Liq. Cryst.*, **73**, 47 (1981).
12. M. Sorai, H. Yoshioka and H. Suga, *Mol. Cryst. Liq. Cryst.*, **84**, 39 (1982).
13. M. Piattelli, E. Fattorusso, R. A. Nicolaus and S. Magno, *Tetrahedron*, **21**, 3229 (1965).
14. P. Le Barney, private communication.
15. J. F. W. McOmie, M. L. Watts and D. E. West, *Tetrahedron*, **24**, 2289 (1968).
16. M. Sorai and K. Kaji, Construction of an adiabatic calorimeter workable between 12 and 530 K, unpublished.
17. M. Sorai and S. Seki, *J. Phys. Soc. Japan*, **32**, 382 (1972).
18. M. Cotrait, P. Marsau, C. Destrade and J. Malthete, *J. Phys. Lett.*, (*Paris*), **40**, L-519 (1979).
19. M. Sorai, K. Tsuji, H. Suga and S. Seki, "*Liquid Crystals*," S. Chandrasekhar, Ed.; Heyden and Son: London, p. 41 (1980).